

# Host–Guest Chemistry from Solution to the Gas Phase: An Essential Role of Direct Interaction with Water for High-Affinity Binding of Cucurbit[*n*]urils

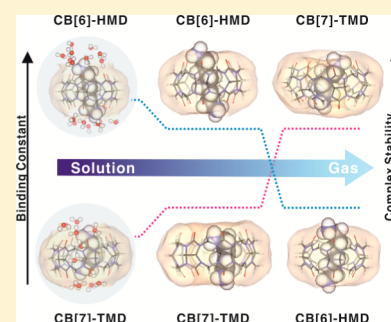
Shin Jung C. Lee,<sup>†</sup> Jong Wha Lee,<sup>†</sup> Hong Hee Lee,<sup>†</sup> Jongcheol Seo,<sup>†</sup> Dong Hun Noh,<sup>†</sup> Young Ho Ko,<sup>§</sup> Kimoon Kim,<sup>†,‡,§</sup> and Hugh I. Kim<sup>\*,†,‡</sup>

<sup>†</sup>Department of Chemistry, <sup>‡</sup>Division of Advanced Materials Science, Pohang University of Science and Technology (POSTECH), Pohang 790-784, Republic of Korea

<sup>§</sup>Center for Self-Assembly and Complexity, Institute for Basic Science, Pohang University of Science and Technology (POSTECH), Pohang 790-784, Republic of Korea

## Supporting Information

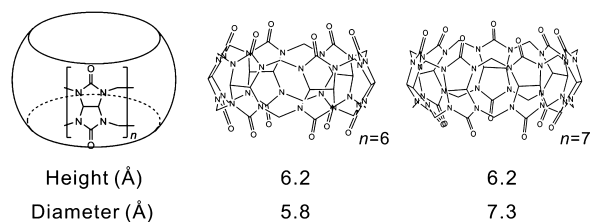
**ABSTRACT:** An investigation of the host–guest chemistry of cucurbit[*n*]uril (CB[*n*], *n* = 6 and 7) with  $\alpha,\omega$ -alkyldiammonium guests ( $\text{H}_2\text{N}(\text{CH}_2)_x\text{NH}_2$ , *x* = 4, 6, 8, 10, and 12) both in solution and in the gas phase elucidates their intrinsic host–guest properties and the contribution of solvent water. Isothermal titration calorimetry and nuclear magnetic resonance measurements indicate that all alkyldiammonium cations have inclusion interactions with CB[*n*] except for the CB[7]–tetramethylenediamine complex in aqueous solution. The electrospray ionization of mixtures of CB[*n*] and the alkyldiammonium guests reflects their solution phase binding constants. Low-energy collision-induced dissociations indicate that, after the transfer of the CB[*n*]–alkyldiammonium complex to the gas phase, its stability is no longer correlated with the binding properties in solution. Gas phase structures obtained from density functional theory calculations, which support the results from the ion mobility measurements, and molecular dynamics simulated structures in water provide a detailed understanding of the solvated complexes. In the gas phase, the binding properties of complexation mostly depend on the ion–dipole interactions. However, the ion–dipole integrity is strongly affected by hydrogen bonding with water molecules in the aqueous condition. Upon the inclusion of water molecules, the intrinsic characteristics of the host–guest binding are dominated by entropic-driven thermodynamics.



## INTRODUCTION

Water-soluble synthetic receptor molecules have been developed and investigated widely due to their numerous potential applications.<sup>1,2</sup> Cucurbit[*n*]urils (CB[*n*], *n* = 5–8, 10) are neutral macrocyclic host molecules that exhibit highly efficient host properties in aqueous solution (Scheme 1).<sup>3–5</sup>

**Scheme 1. Structure of CB[*n*] (*n* = 6, 7)**



Two carbonyl-laced portals bind positively charged functional groups of guest molecules with ion–dipole interactions.<sup>4–6</sup> The hydrophobic interaction in the cavity of CB[*n*] provides entropic gain with water release from the cavity upon the inclusion of the guest molecule.<sup>5,7–9</sup> Because of these unique characteristics, CB[*n*] molecules have been used as highly

effective host molecules in molecular recognition and sensing,<sup>10–14</sup> the construction of supramolecular architectures,<sup>15,16</sup> drug/gene delivery systems,<sup>17–19</sup> and various biological applications such as the probing and controlling of protein structures.<sup>20–23</sup>

Size complementarity of the guest molecule to the rigid structured CB[*n*] also plays an important role in the exceptional binding properties of CB[*n*] molecules.<sup>4</sup> CB[5], which has the smallest cavity size (4.4 Å inner diameter), can encapsulate a small guest such as O<sub>2</sub> and N<sub>2</sub>.<sup>24</sup> CB[6] has a larger cavity (5.8 Å inner diameter), which allows the binding of various guests of appropriate length and size, such as  $\alpha,\omega$ -alkyldiammonium guests.<sup>25–27</sup> The complex shows a pseudorotaxane structure, where each ammonium group interacts with each carbonyl-laced portal while the alkyl group threads through CB[6].<sup>26</sup> CB[7] also shows the formation of pseudorotaxane structures with polyaromatic diammonium cations. In addition, CB[7] exhibits a high binding affinity to bicyclo[2.2.2]octane, adamantane, and ferrocene molecules

**Received:** May 31, 2013

**Revised:** June 19, 2013

**Published:** June 26, 2013

with ammonium groups because of its relatively larger cavity size (7.3 Å inner diameter).<sup>10,28,29</sup>

Fewer studies have considered the intrinsic host–guest properties of solvation free CB[n] complex systems.<sup>30–36</sup> A few studies have reported that the solution phase host–guest interactions of CB[n] can survive even after the CB[n] complexes are transferred to the gas phase via electrospray ionization (ESI).<sup>35–40</sup> For example, Scherman and co-workers reported a similar trend between ESI abundances and the binding properties in solution with tertiary complexes of CB[8] with methyl viologens and electron-rich guest molecules.<sup>35,36</sup> Dearden and co-workers have reported that the pseudorotaxane structures of CB[6]–diammonium complexes are preserved even after desolvation.<sup>31,32,34,37</sup> Also, they have studied the structure selectivity of CB[6] toward *para*-phenylenediamine and the molecular trap of CB[6] and CB[7] complexes capped with two guanidinium ions.<sup>37</sup> Recently, CB[7]–bisimidazolium salt complexation and dication encapsulation with CB[8] were probed using ESI-MS.<sup>39,40</sup> Several studies of the unique gas-phase reactions of guest molecules in the CB[n] complexes have also been published.<sup>38,41–43</sup>

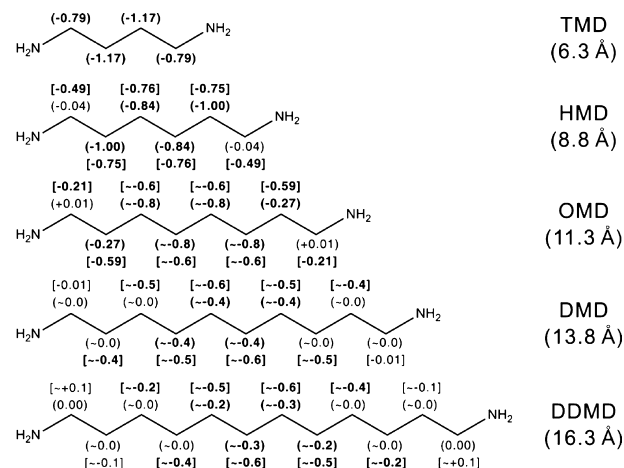
Although several studies have shown that the solution-phase properties of CB[n] complexes can be transferred to the gas phase, the gas-phase stabilities of CB[n] complexes are generally different from their solution-phase binding properties.<sup>31–33</sup> In contrast to the solution phase, hydrophobic interaction, which is one of the key interactions for the host–guest chemistry of CB[n],<sup>8,9</sup> is no longer available in the gas phase. Moreover, water molecules are expected to play an important role in ion–dipole interactions between the host and the guest. These differences would result in a difference in the specific recognition of CB[n] from the solution to the gas phase. As of yet, no detailed studies of the solution-phase host properties of CB[n], which are directly related to interactions with solvent water, compared with its intrinsic host properties in the absence of water solvent have been reported. In the present study, we report on the host–guest interactions of CB[6] and CB[7] with a series of  $\alpha,\omega$ -alkyldiamine ( $\text{H}_2\text{N}-(\text{CH}_2)_x\text{NH}_2$ ,  $x = 4, 6, 8, 10, \text{ and } 12$ , Scheme 2) in both solution and gas phase. By comparing the solution-phase structures and binding properties of the CB[n]–alkyldiammonium complexes to their gas-phase structures and complex stabilities, we investigated the contribution of the water solvation shell at the CB[n] portal to the complicated host–guest interactions in the solution. Of particular interest is the size complementarity of  $\alpha,\omega$ -alkyldiammonium guests relative to the cavity sizes of CB[6] and CB[7].

## MATERIALS AND METHODS

**Materials.** CB[6], CB[7], and formic acid were purchased from Sigma-Aldrich (St. Louis, MO, USA), and all  $\alpha,\omega$ -alkyldiammoniums were purchased from Tokyo Chemical Industry Co. (Tokyo, Japan). HPLC grade water was used as a solvent and purchased from J. T. Baker (Phillipsburg, NJ, USA). CB[6] and CB[7] stock solutions (2 mM) are prepared in 60% formic acid.

**Isothermal Titration Calorimetry.** Isothermal titration calorimetry (ITC) experiments are conducted using a VP-ITC calorimeter (Microcal, Norhampton, MA, USA). The reference cell is filled with 50% formic acid, and 0.2 mM alkyldiammoniums are dissolved in 50% formic acid and loaded in the ITC cell. Three millimolar CB[n] in 50% formic acid with a volume of 6  $\mu\text{L}$  is injected into a solution of alkyldiammonium 40

**Scheme 2. Structures of  $\alpha,\omega$ -Alkyldiamines and Relative Chemical Shifts ( $\Delta\delta$ , ppm) upon Complexation with CB[6] (Round Brackets) and CB[7] (Square Brackets) from  $^1\text{H}$  NMR Spectra<sup>a</sup>**



<sup>a</sup>The length is the nitrogen–nitrogen distance.  $\Delta\delta$  values greater than 0.2 were bolded to note extensive shifts. TMD has a low binding affinity toward CB[7] in solution, and chemical shifts upon complexation with CB[7] are not observed.

times. For CB[7] titration of DDMD, 2 mM alkyldiammonium solution with 50% formic acid is used, and the concentration of the injectant is set at 30 mM. The interval time is adjusted to 180 s with stirring at 502 rpm, and the cell temperature is maintained at 25 °C.

**NMR Spectroscopy.**  $^1\text{H}$  NMR spectra are recorded with a Bruker AVANCE 300 MHz spectrometer (Bruker BioSpin Co., Billerica, MA, USA). Formic acid/ $\text{D}_2\text{O}$  (30/70 v/v) is used as the solvent, and the sample concentration is in the range 0.5–3 mM. Data analyses are performed with Spinworks 3.

**Electrospray Ionization Traveling Wave Ion Mobility Mass Spectrometry.** Gas phase experiments are performed on a Waters Synapt G2 HDMS traveling wave ion mobility orthogonal acceleration time-of-flight mass spectrometer (Waters, Manchester, U.K.) in positive ion mode. A source temperature of 100 °C, capillary voltage of 3.50 kV, desolvation temperature of 250 °C, and cone voltage of 40 V are set as parameters for ESI. Helium cell flow rate is set as 180 mL/min. Nitrogen drift gas is introduced to the traveling wave ion mobility cell at a 60 mL/min flow rate. The optimized traveling wave (T-wave) height and velocity are 11 V and 300 m/s, respectively. For each sample, 101 spectra are obtained and averaged for analysis. The drift times of analyte ions are determined from the location of the ion mobility peak maxima extracted using MassLynx (version 4.1) software (Waters, Milford, MA, USA). ESI-MS spectra of the diluted CB[6] and CB[7] solutions are tested before  $\alpha,\omega$ -alkyldiammonium is added. Doubly protonated CB[6] and CB[7] ions are observed as the predominant peak in the ESI-MS spectra. Then, a stoichiometric amount of  $\alpha,\omega$ -alkyldiammonium is added. The final concentration for the ESI is adjusted to 20  $\mu\text{M}$  (CB[n]: $\alpha,\omega$ -alkyldiammonium = 1:1 with 2% (v/v) formic acid). For analyzing the complex formation of CB[n] with two alkyldiammonium ions, mixing two alkyldiammonium solutions is prior to addition of CB[n] solution. The final concentration of two alkyldiammonium and CB[n] is 20  $\mu\text{M}$ , and ESI

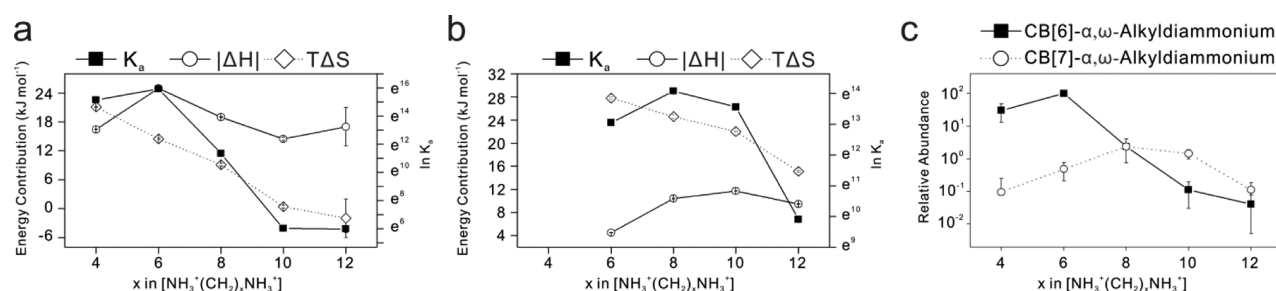


**Figure 1.** ITC measured  $K_a$  and enthalpic and entropic gains of (a) CB[6] and (b) CB[7] upon complex formation with  $\alpha,\omega$ -alkyldiammonium guests. (c) ESI-MS measured relative abundance of CB[6] and CB[7] complexes with  $\alpha,\omega$ -alkyldiammonium guests.

experiments of one alkyldiammonium with two CB[ $n$ ] are conducted in the same manner.

**Collision-Induced Dissociation.** Collision-induced dissociation experiments to estimate gas phase complex stability are performed in a Waters Synapt G2 HDMS quadrupole time-of-flight mass spectrometer and Thermo Scientific LTQ Velos ion trap mass spectrometer (Thermo Scientific, San Jose, CA, USA). The electrospray parameter and experimental condition in the Waters Synapt G2 are the same as stated above in the normal ESI experiment. In the LTQ Velos ion trap, the sample injection rate is adjusted to 5  $\mu\text{L}/\text{min}$ , and the electrospray voltage and capillary temperature are set to 3.5 kV and 250  $^\circ\text{C}$ . Spectra for all samples are collected over 100 scans and averaged, and then analyzed using Thermo Xcalibur 2.1 software (Thermo Scientific, San Jose, CA, USA).

**DFT Calculations.** The structures and energetics of the CB[ $n$ ]-alkyldiammonium ions in the gas phase are determined by density functional theory (DFT) calculations using Q-Chem 3.2 (Q-Chem Inc., Pittsburgh, PA, USA) with the Becke's three-parameter functional (B3) combined with the correlation function of Lee, Yang, and Parr (LYP).<sup>44–46</sup> More than 2000 possible molecular conformations are searched for candidate complex structures using HyperChem 7.5 (Hypercube Inc., Gainesville, FL, USA). A total of six final candidate structures are selected for the DFT calculations among the 50 candidates after optimization using an AMBER force field. The structures are optimized using the 6-31G basis set, and the final energies are calculated using the 6-31G(d,p) basis set.<sup>47–49</sup>

**MD Simulations.** All MD simulations are performed with Gromacs 4.5.5.<sup>50</sup> The force field parameters for the alkyldiammonium cations are taken from the force field parameters for the lysine group in the AMBER99SB force field.<sup>51</sup> The model for CB[ $n$ ] is prepared following the previously reported method.<sup>8</sup> Briefly, the atoms of CB[ $n$ ] are restrained during the simulation, and the partial atomic charges are taken from the DFT calculations with the B3LYP/6-31G(d) basis set. The Lennard-Jones parameters are adopted from the fluorine atom to account for the polarizability of the CB[ $n$ ] cavity.<sup>8,52</sup> The simulations are carried out with approximately 1300 water molecules (TIP3P) in a triclinic box using the particle mesh Ewald<sup>53</sup> for long-range electrostatic treatment and a Berendsen thermostat and barostat to maintain the temperature and pressure.<sup>54</sup> Additional simulations with the TIP4P-Ew water model also show good agreement with the simulations with the TIP3P water model (Table S6, Supporting Information).

## RESULTS AND DISCUSSION

**Thermodynamics of CB[ $n$ ]-Alkyldiammonium Complexes in the Solution Phase.**  $\alpha,\omega$ -Alkyldiammonium guests

have different binding affinities to CB[ $n$ ] based on their alkyl chain lengths.<sup>26,31</sup> Five  $\alpha,\omega$ -alkyldiammoniums with different alkyl chain lengths, which are tetramethylenediamine (TMD,  $x = 4$ ), hexamethylenediamine (HMD,  $x = 6$ ), 1,8-octamethylenediamine (OMD,  $x = 8$ ), 1,10-decamethylenediamine (DMD,  $x = 10$ ), and 1,12-dodecamethylenediamine (DDMD,  $x = 12$ ), are investigated (Scheme 2). Isothermal titration calorimetry (ITC) is utilized to investigate the binding events of CB[6] and CB[7] to a series of doubly protonated  $\alpha,\omega$ -alkyldiammonium guests in aqueous solution with formic acid (50% by volume). ITC measurements indicate that all of the alkyldiammonium guests have single binding to CB[6] and CB[7] (Figure S1, Supporting Information), except for CB[7]–TMD. As shown in Figure 1a, CB[6]–HMD shows the strongest binding affinity among all the complexes investigated in the present study, with an equilibrium association constant ( $K_a$ ) of  $8.2 \times 10^6 \text{ M}^{-1}$ . Strong binding between CB[6] and TMD is also observed ( $K_a = 3.8 \times 10^6 \text{ M}^{-1}$ ). The  $K_a$  of the CB[6]-alkyldiammonium complexes decreases as the alkyl chain length increases. The observed binding properties of the CB[6]-alkyldiammonium complexes agree with previous reports on their binding properties in various aqueous solutions.<sup>26,55,56</sup> CB[7] shows distinct binding events with the alkyldiammonium guests compared with CB[6] (Figure 1b). Except for TMD, all the alkyldiammonium guests investigated in the present study show strong binding with CB[7] ( $K_a > 10^4 \text{ M}^{-1}$ ). Nevertheless, there is also a decreasing trend of  $K_a$  with an increasing chain length for the guests longer than OMD. The binding constant between CB[7] and TMD is not measurable by ITC. We infer that the CB[7] and TMD interaction is much weaker than the ITC measurable strength ( $K_a < 10^2 \text{ M}^{-1}$ ).

Thermodynamic values (Table 1) of CB[6] complex formations with alkyldiammonium guests indicate that the distinct  $K_a$  for each alkyldiammonium guest is largely due to enthalpic gain (Figure 1a). Nevertheless, a significant decrease of the  $K_a$  with the increasing chain length of the guests is attributed to the decrease in entropic gain upon complex formation. Even entropic loss is observed with the longest guest (i.e., DDMD). The complexation process, in terms of entropy, can be characterized by two events: entropic gain by the release of water molecules that originally occupy the CB[ $n$ ] cavity and entropic loss by the adjoining of two independent molecules. Because entropic gain can only be obtained from water release from the cavity and the portals, the observed entropic gain for all of the CB[6]-alkyldiammonium complexes, except for DDMD, suggests an inclusion of the guest molecules into the cavity. The observed decrease in entropic gain with the increase in the chain length is attributed to the enlarged entropic loss of the guest molecule upon complexation due to the restricted freedom of motion. The alkyldiammonium guests longer than



**Table 1.** ITC Measured Thermodynamic Values of CB[*n*] Complexes with  $\alpha,\omega$ -Alkyldiammonium Guests at 298 K

host	guest	$K_a$ ( $M^{-1}$ )	$\Delta H$ (kJ mol $^{-1}$ )	$-T\Delta S$ (kJ mol $^{-1}$ )
CB[6]	TMD	$3.8 (\pm 0.2) \times 10^6$	$-16.45 \pm 0.03$	$-21.1 \pm 0.1$
	HMD	$8.2 (\pm 0.4) \times 10^6$	$-24.99 \pm 0.04$	$-14.5 \pm 0.1$
	OMD	$8.5 (\pm 0.9) \times 10^4$	$-19.00 \pm 0.04$	$-9.1 \pm 0.3$
	DMD	$4.12 (\pm 0.04) \times 10^5$	$-14.5 \pm 0.3$	$-0.4 \pm 0.3$
	DDMD	$4 (\pm 1) \times 10^2$	$-17 \pm 4$	$2 \pm 4$
CB[7]	TMD	NA	NA	NA
	HMD	$4.7 (\pm 0.3) \times 10^5$	$-4.49 \pm 0.02$	$-27.8 \pm 0.2$
	OMD	$1.3 (\pm 0.1) \times 10^6$	$-10.40 \pm 0.06$	$-24.6 \pm 0.3$
	DMD	$7.8 (\pm 0.3) \times 10^5$	$-11.72 \pm 0.03$	$-22.0 \pm 0.1$
	DDMD	$2.0 (\pm 0.1) \times 10^4$	$-9.45 \pm 0.06$	$-15.1 \pm 0.1$

HMD ( $x > 6$ ) show stronger binding to CB[7] than to CB[6], despite their lower enthalpic gain (Table 1, Figure 1b). In contrast to CB[6], the overall complex formation of CB[7] is dependent on entropic gain. Despite having a larger number of internal water molecules in the CB[7] cavity than in that of CB[6], recent studies indicate that the entropic gain from water release is smaller for CB[7] than for CB[6] upon complex formation.<sup>8</sup> However, occupied alkyl chains are exposed to smaller barriers to their freedom of motion in CB[7] than in CB[6]. Similarly, the entropic gain for CB[7] is lowered upon complex formation as the length of the alkyldiammonium guests is increased. In contrast, the enthalpic gains are greater in CB[6] complexes compared to those in CB[7] complexes. The value of the enthalpic gain suggests a more favorable electrostatic interaction of the guest in CB[6] than in CB[7]. Particularly, HMD shows enhanced enthalpic gain upon complex formation with CB[6]. It is inferred that the size of HMD is appropriate to allow both ammonium groups to interact strongly with the carbonyl groups of the CB[6] portals in solution.

**Host–Guest Interactions of CB[*n*]–Alkyldiammonium Complexes in Solution.** The  $^1H$  NMR spectroscopy measurements indicate that the alkyldiammoniums form stable 1:1 complexes with CB[6] and CB[7], consistent with thermodynamic data from ITC measurements. The upfield shift of the methylene hydrogens from the original chemical shift ( $\Delta\delta$ ) of the free alkyldiammonium guest indicates the inclusion of the alkyl chain into the CB[*n*] cavity (Scheme 2).<sup>7,26</sup> Similar to the ITC results, no upfield shift is found from CB[7]–TMD, indicating that TMD does not form a stable complex with CB[7] in aqueous solution. Overall, all of the alkyldiammonium guests, other than CB[7]–TMD, are internally bound to CB[*n*]. Large shifts of all the methylene hydrogens of TMD with CB[6] ( $\Delta\delta = -0.79$  and  $-1.17$  ppm) indicate complete and tight inclusion of TMD. For the other alkyldiammonium guests, four methylene groups in the middle of alkyl chains usually experience large shifts upon complexation with CB[6]. The upfield chemical shifts upon complexation are almost the same as those reported by Mock and Shih.<sup>26</sup>

In the case of CB[7] complexes, more methylene groups of the alkyldiammonium guests experience upfield shifts from the

original  $\delta$ , indicating that a greater number of the methylene groups are incorporated into the CB[7] cavity. Except for the two longest guests ( $x = 10$  and 12), the entire alkyl chains of the guests experience shifts in  $\delta$ . For DMD and DDMD, eight methylene groups show large shifts due to their greater interaction with the CB[7] cavity. Upfield shifts of more methylene groups indicate participation of a greater portion of the alkyl chain in hydrophobic interactions with CB[7]. It is inferred that CB[7] can provide more space for the guests to fluctuate inside the cavity. This is in line with CB[7] having a larger cavity diameter than CB[6].

**ESI-MS Reflects the Host–Guest Chemistry of CB[*n*]–Alkyldiammonium Complexes in Solution.** Combined with mass spectrometry (MS), ESI has been widely used to investigate the intrinsic properties of supramolecular complexes in the absence of solvent because of its ability to transfer ions from solution to the gas phase intact.<sup>31–36</sup> The ESI-MS spectrum of a stoichiometric (1:1 by mol) mixture of CB[6] and  $\alpha,\omega$ -alkyldiammonium shows the doubly charged CB[6] complex ion as the dominant species in the spectrum (Figure S2a, Supporting Information). The ESI-MS spectrum of a mixture of CB[7] and  $\alpha,\omega$ -alkyldiammonium (1:1 by mol) shows the doubly charged CB[7]–alkyldiammonium complex ion as the dominant species (Figure S2b, Supporting Information).

We investigate the correlation between the relative abundances of the complex ions from ESI and their  $K_a$  in solution. To compare the relative abundances of CB[*n*] complex species in the ESI-MS spectra, we perform the competition experiment with five alkyldiammonium guests and CB[*n*] (Figure S3, Supporting Information), in the similar way as the previous report.<sup>57</sup> However, it is hard to detect and quantify the relative abundances of the complexes with low  $K_a$ , such as CB[6]–DDMD and CB[7]–TMD, so we modify the method by examining a series of mixtures of equimolar amounts of two different alkyldiammonium guests with CB[*n*] (1:1:1 by mol, Figure S4, Supporting Information). The relative abundances of the  $\alpha,\omega$ -alkyldiammonium complexes of CB[6] and CB[7] are further studied using five mixtures of the alkyldiammonium ( $x = 4, 6, 8, 10$ , and 12) with CB[6] and CB[7] (1:1:1 by mol, Figure S5, Supporting Information). Figure 1c shows the combined relative abundances of the CB[*n*] complexes with the alkyldiammonium guests observed from the ESI-MS spectra. The relative abundances of the CB[6] complex ions with the alkyldiammonium guests correlate well with their solution-phase  $K_a$  values (HMD > TMD > OMD > DMD > DDMD, Figure 1a,c). The observed relative abundances of the complex ions from equimolar amounts of CB[7] and two alkyldiammonium guests (Figure S4b, Supporting Information) also show a good correlation with their solution-phase  $K_a$  values (OMD > DMD > HMD > DDMD > TMD). The finding that CB[7]–TMD is the least abundant complex among all the complex ions indicates that CB[7]–TMD has the weakest binding properties in solution.

Although our ESI results reflect the solution phase properties of host–guest interactions, the relative abundances of the CB[*n*]–alkyldiammonium complexes show some deviations compared with their relative  $K_a$  in solution. The overall differences in the relative abundances of the CB[6] and CB[7] complexes of the longer alkyldiammonium guests (OMD, DMD, and DDMD) become smaller than the  $K_a$  differences in solution. For example, the relative abundances of CB[6]–OMD and CB[7]–OMD are comparable despite their

difference in  $K_a$  in solution. Although the overall binding properties of the complexes are preserved during the ESI processes, the observed minor changes in the relative abundances of the complex ions are induced by the absence of the water solvent.

**Stabilities of CB[n]–Alkyldiammonium Complexes in the Gas Phase.** Low-energy collision-induced dissociation (CID) of each complex ion is utilized to examine the complex stabilities in the gas phase. The experiments are conducted in quadrupole time-of-flight (Q-TOF) and ion trap mass spectrometers for comparison purposes. The CID spectra obtained from the Q-TOF and ion trap are shown in Figures S6 and S7 (see the Supporting Information). The major dissociation product ions found in the CID spectra are the singly protonated diammonium ( $[\text{H}_2\text{N}(\text{CH}_2)_x\text{NH}_2 + \text{H}]^+$ ) and its ammonia-loss fragment in Q-TOF and CB[n] with a proton ( $[\text{CB}[n] + \text{H}]^+$ ) or CB[n] with an ammonia-loss fragment in the ion trap, suggesting that there are two different pathways for the host–guest dissociation in the gas phase: proton- and ammonium-transfer dissociations. The ammonium-transfer dissociation is predominant for TMD, HMD, and OMD, whereas both the proton and ammonium transfers are found for the guests with long alkyl chains, such as DMD and DDMD. The survival yield of the doubly protonated CB[n]–alkyldiammonium complex ion obtained by the energy-dependent CID in the Q-TOF is shown in Figure 2. The

dissociation of CB[6]–alkyldiammonium, showing the highest gas-phase stability for CB[6]–TMD.<sup>31</sup>

These gas-phase stabilities obtained from the dissociation processes cannot be quantitatively correlated with the gas-phase host–guest binding energy, because two different dissociation pathways, proton- and ammonium-transfer dissociations, whose contributions depend on the alkyl chain length of the diammonium guests, make a direct comparison between the binding strengths of the complex ion with various guests impossible. However, the trends are believed to be the same in the obtained gas-phase stability and the gas-phase host–guest binding energy. The CID spectrum suggests that the proton-transfer dissociation requires far higher energy than the ammonium-transfer dissociation for TMD, HMD, and OMD. Moreover, the relative abundance of singly protonated diammonium generated by the proton-transfer dissociation gradually increases as the alkyl chain length increases from OMD to DDMD at the same collision energy. These results indicate that the threshold energy for the proton-transfer dissociation of the CB[n]–alkyldiammonium complex continuously decreases as the alkyl chain length of the diammonium guest increases, and thus, it follows the trend of the observed gas-phase stability. Although the proton-transfer dissociation has a somewhat higher activation barrier than the gas-phase host–guest binding energy, it is expected to follow the trend of gas-phase binding energy and might be the best measure in our experimental setup. Thus, the binding energy of the CB[n]–alkyldiammonium complex ion in the gas phase is expected to have the following trend: TMD > HMD > OMD > DMD > DDMD. Note that this trend is different from that in the presence of solvent.

In the absence of solvent water, direct ion–dipole interactions between the ammonium groups of the guest and the carbonyl groups of the CB[n] become an essential driving force to stabilize the complex. It is inferred that two short alkyldiammonium guests (TMD and HMD) fit the cavity height (6.2 Å) of CB[6] in the absence of water, so both ammonium groups interact with both carbonyl-laced portals of CB[n] with relatively small structural distortion of the guest. However, for long alkyldiammonium guests (OMD, DMD, and DDMD), resistance to the strong ion–dipole interactions between the guest and the host due to the structural distortion induced by the excess length of the guest alkyl chain is thought to be the cause of the observed low stabilities of their CB[n] complexes.

**Structures of CB[n]–Alkyldiammonium Complexes in the Gas Phase.** Gas-phase structures of the CB[n] complexes with  $\alpha,\omega$ -alkyldiammonium guests are investigated using traveling wave ion mobility spectrometry (TWIMS) combined with computational calculations (Figure 3). Theoretically calculated collision cross section ( $\Omega_D$ ) values from the optimized complex structures based on the density functional theory (DFT) calculations are compared with the experimental  $\Omega_D$  values of the complex ions using calibration methods.<sup>58</sup> The experimental  $\Omega_D$  values of all of the complex ions show overall agreement with the theoretical  $\Omega_D$  values of the threaded structures, with an average deviation of 1.6% (Table S1, Supporting Information). Representative structures of CB[n]–alkyldiammonium obtained from the DFT calculations are shown in Figure 3 as insets (see Figures S9 and S10 in the Supporting Information for additional DFT-optimized structures). For the CB[6]–alkyldiammonium complex ions, the threaded structures of the complex ions are significantly lower

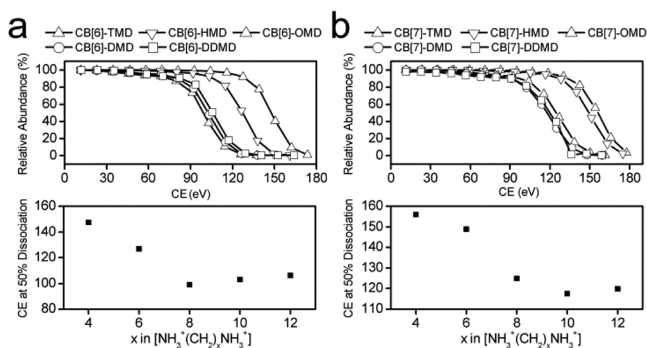


**Figure 2.** (top) Plots of the fraction of TMD, HMD, OMD, DMD, and DDMD complexes of (a) CB[6] and (b) CB[7] as a function of collision energy (CE). (bottom) Relative energies for 50% loss of each complex ion plotted as points with error bars as one standard deviation. All collision energy is expressed in the center-of-mass frame.

survival yields for the CB[6] and CB[7] complexes of various  $\alpha,\omega$ -alkyldiammoniums show similar slopes for all guests, regardless of their alkyl chain lengths. Thus, the relative energy for the 50% loss of each complex ion is determined by the linear fitting of the falling portion of the curve and is used to compare the relative stabilities of the complex ions (Figure 2). Of the alkyldiammonium guests, the CB[n]–TMD complex ion shows the highest gas-phase stability for both CB[6] and CB[7], and the stability gradually decreases as the chain length of the guest increases up to OMD. For OMD, DMD, and DDMD, the gas-phase stability is nearly constant, regardless of the chain length. In summary, the observed gas-phase stability of the CB[n]–alkyldiammonium complex follows the trend TMD > HMD > OMD  $\approx$  DMD  $\approx$  DDMD for both CB[6] and CB[7]. These results are in agreement with the study with the ion trap (Figure S8, Supporting Information) and a previously reported study by Dearden and co-workers using sustained off-resonance irradiation CID (SORI-CID) for the gas-phase

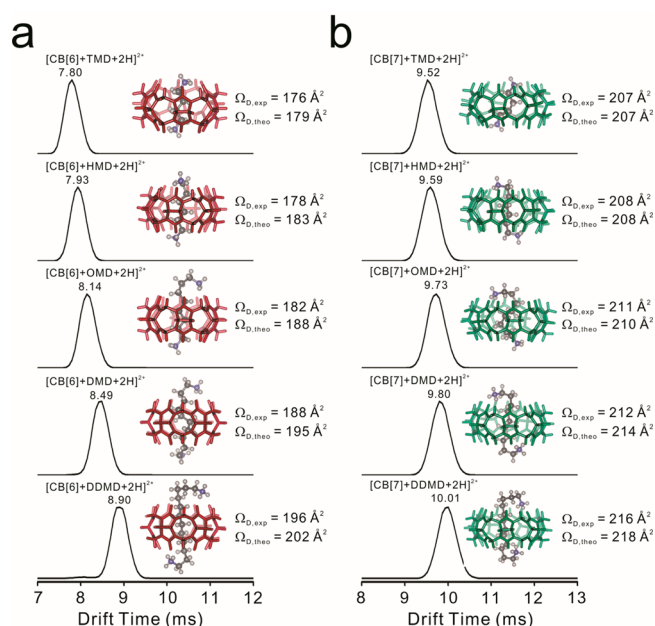


**Figure 3.** Arrival time distributions of doubly charged TMD, HMD, OMD, DMD, and DDMD complexes of (a) CB[6] and (b) CB[7] from TWIMS. The theoretically calculated structure and  $\Omega_D$  for each complex ion are also shown as the right inset.

in energy than the externally bound structures by approximately 68–126 kJ mol<sup>−1</sup>. The CB[7]–alkyldiammonium complex ions also energetically prefer the threaded structures over the externally bound structures.

The DFT-calculated structures provide detailed information related to the observed tendency of the stabilities of the complex ions. Because of the small cavity size of CB[6] (i.d. approximately 5.8 Å), the excess length of the alkyl chain portion of the guest sticks out from the host to allow the ammonium groups to interact with the carbonyl groups at the portals (Figure 3a). There is a somewhat larger space inside CB[7] (i.d. approximately 7.3 Å) (Figure 3b). In addition, the diameter of the carbonyl-laced portals is larger in CB[7] than in CB[6]. Two distinct structural features are observed from the CB[7]–alkyldiammonium complex structures compared with structures of the CB[6]–alkyldiammonium complexes. First, due to the larger cavity size, the alkyl chain of the alkyldiammonium can adjust its conformation to allow both

ammonium groups to interact with the carbonyl groups at each portal of CB[7], as discussed earlier. In addition, the excess portions of the alkyl chain of the alkyldiammonium ion stick out from both sides of CB[7] as a bent structure.  $\alpha,\omega$ -Alkyldiammonium guests longer than HMD have weak interactions with CB[*n*] via bending of the alkyl chain from outside the CB[*n*]. As a result, all three long alkyldiammonium guests ( $x = 8, 10$ , and  $12$ ) exhibit lower stabilities than the shorter guests in both CB[6] and CB[7] (Figure 3). HMD shows a significantly lower stability than TMD with CB[6] in the gas phase, whereas a similar stability is observed with CB[7]. The total length of HMD (8.8 Å) is greater than the distance between the carbonyl groups of one portal to the other of CB[*n*] (6.2 Å). This length difference causes weaker interactions between the ammonium group of HMD and the carbonyl group of CB[6] in the absence of water solvent, because the small cavity size of CB[6] prevents HMD from adjusting its structure to increase the ion–dipole interactions (Figure S10, Supporting Information). The relatively larger cavity size of CB[7] allows the ammonium groups of HMD to be bent to interact with the carbonyl group as strongly as those of TMD.

#### Essential Role of Water for High-Affinity Host–Guest Chemistry of CB[*n*] with $\alpha,\omega$ -Alkyldiammonium Guests.

In the present study, the difference in the host–guest interaction affinities of CB[*n*] to  $\alpha,\omega$ -alkyldiammonium guests from the aqueous solution to the gas phase is demonstrated. Understanding the role of water solvent is essential for designing efficient host–guest strategies in the aqueous phase. Both enthalpic gain from ion–dipole interactions and entropic gain from hydrophobic interactions are key factors for the host–guest interactions of CB[*n*] in aqueous solution. Strong binding between CB[*n*] and a guest can be achieved from size complementarity between the host and the guest, which optimizes both the hydrophobic and ion–dipole interactions. To understand how size complementarity is determined in aqueous solution, we perform molecular dynamics (MD) simulations of the CB[*n*]–alkyldiammonium complex systems in TIP3P and TIP4P-Ew water solvent.

The importance of enthalpic gain upon CB[6]–alkyldiammonium complex formation is observed from the ITC measurements. The computed interaction between CB[6] and the alkyldiammonium cation decreases as the chain length of the alkyldiammonium cation decreases (Table 2). The

**Table 2.** Calculated Coulomb Potential and Lennard-Jones Potential Energy (kJ mol<sup>−1</sup>) between CB[*n*] (*n* = 6, 7), Diammonium (DA), and Solvent and Ions (Sol) from MD Simulations<sup>a</sup>

	energy	TMD	HMD	OMD	DMD	DDMD
CB[6]	$E_{\text{Coul}}(\text{CB}[n]-\text{DA})$	$-214.2 \pm 14.1$	$-166.7 \pm 15.2$	$-104.5 \pm 23.1$	$-75.6 \pm 21.9$	$-61.5 \pm 21.5$
	$E_{\text{LJ}}(\text{CB}[n]-\text{DA})$	$-36.7 \pm 9.3$	$-52.2 \pm 8.3$	$-59.2 \pm 8.1$	$-65.1 \pm 7.2$	$-66.8 \pm 7.6$
	$E_{\text{Coul}}(\text{CB}[n]-\text{sol})$	$-193.5 \pm 31.0$	$-208.3 \pm 32.1$	$-251.6 \pm 36.1$	$-275.0 \pm 36.4$	$-286.2 \pm 36.2$
	$E_{\text{LJ}}(\text{CB}[n]-\text{sol})$	$-146.8 \pm 14.2$	$-140.5 \pm 14.8$	$-130.2 \pm 15.9$	$-125.4 \pm 16.1$	$-123.3 \pm 16.1$
	$E_{\text{Coul}}(\text{DA}-\text{sol})$	$-128.3 \pm 24.6$	$-169.3 \pm 30.1$	$-227.9 \pm 37.4$	$-240.9 \pm 34.9$	$-247.0 \pm 34.2$
	$E_{\text{LJ}}(\text{DA}-\text{sol})$	$6.7 \pm 9.5$	$4.2 \pm 11.5$	$2.3 \pm 13.5$	$-10.0 \pm 13.5$	$-23.7 \pm 13.8$
CB[7]	$E_{\text{Coul}}(\text{CB}[n]-\text{DA})$	NA	$-105.6 \pm 18.7$	$-83.4 \pm 23.1$	$-70.6 \pm 21.9$	$-54.1 \pm 22.6$
	$E_{\text{LJ}}(\text{CB}[n]-\text{DA})$	NA	$-46.6 \pm 5.6$	$-54.4 \pm 5.5$	$-61.4 \pm 6.7$	$-67.2 \pm 7.3$
	$E_{\text{Coul}}(\text{CB}[n]-\text{sol})$	NA	$-314.3 \pm 37.5$	$-324.7 \pm 38.7$	$-332.6 \pm 38.9$	$-346.4 \pm 39.3$
	$E_{\text{LJ}}(\text{CB}[n]-\text{sol})$	NA	$-150.1 \pm 17.5$	$-146.0 \pm 17.4$	$-142.9 \pm 17.5$	$-139.4 \pm 17.6$
	$E_{\text{Coul}}(\text{DA}-\text{sol})$	NA	$-242.2 \pm 35.7$	$-248.9 \pm 36.9$	$-248.1 \pm 34.7$	$-255.3 \pm 34.6$
	$E_{\text{LJ}}(\text{DA}-\text{sol})$	NA	$16.5 \pm 13.9$	$6.2 \pm 13.6$	$-4.8 \pm 13.5$	$-15.7 \pm 13.8$

<sup>a</sup>The values are averaged over 2001 frames of a 10 ns simulation, and the errors are standard deviations.



decrease in the interactions between the host and the guest originates from the decrease in the Coulombic energy from ion–dipole interactions between the ammonium groups of the guest and the carbonyl groups of the host. This is also reflected in the number of hydrogen bonds (Table S2, Supporting Information). All three of the long alkyldiammonium guests ( $x = 8, 10,$  and  $12$ ) have approximately 0.5 hydrogen bonds with the carbonyl oxygen of CB[6], whereas the two shorter guests (TMD and HMD) have approximately 3.2 and 1.8 hydrogen bonds, respectively. However, the decrease in the interaction between CB[6] and the alkyldiammonium cations is compensated for by the interaction with the solvent water molecules (Figure 4). More hydrogen bonds with solvent water

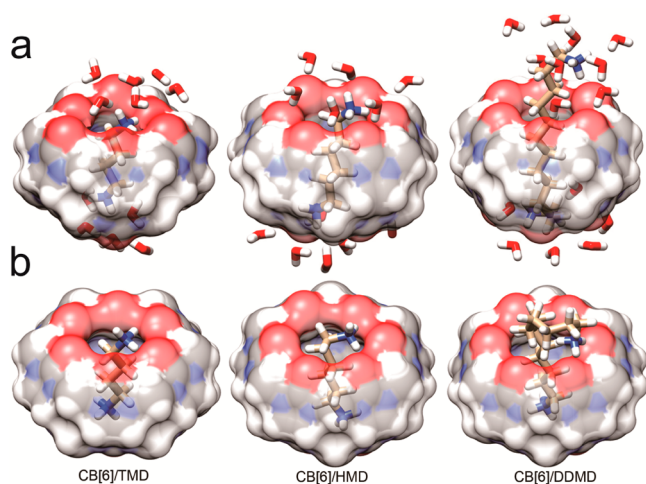


**Figure 4.** (a) The representative snapshots of CB[6]–TMD, CB[6]–HMD, and CB[6]–DDMD from 10 ns MD simulations in a water box and (b) the structure of CB[6]–TMD, CB[6]–HMD, and CB[6]–DDMD from DFT calculations *in vacuo*.

are formed with an increase in the chain length of the guest and a decrease in the interactions with the host (Table S2, Supporting Information). As a result, the total number of hydrogen bonds and the enthalpic gain of the ammonium groups are comparable for all of the guests, except for HMD, upon complex formation with CB[6]. The ITC measurements show that CB[6]–HMD complexation causes an exceptionally large enthalpic gain, which can be explained by an increase in the van der Waals interactions between the host and the guest.<sup>55</sup> Although the force field energetics does not directly correspond to the experimentally measured enthalpies, a correlation can be assumed.<sup>8</sup> The Lennard-Jones potential has an increasing trend with the increasing chain length, which implies an increase in van der Waals interactions between CB[6] and HMD, compared to CB[6] and TMD (Table 2). Water molecules, which directly interact with the solute, are essential for the energetic and structural aspects of the solute in the solution.<sup>59,60</sup> In the aqueous solution, electronegative carbonyl-laced portals and the electropositive outer surface of CB[6] are expected to interact directly with water molecules. Even upon complex formation with TMD, its structural rigidity may be preserved by interactions with water.

This is different from the theoretical structure, in which the carbonyl groups in both portals are shrunk inward to maximize the ion–dipole interactions with TMD. Thus, we think that the short length of TMD may limit its strong interactions to one of the portals or allow weak interactions with both portals of the

rigid CB[6] in solution. The observed difference between the  $K_a$  in the solution and gas-phase complex stability is attributed to the interaction of the guest with water. In aqueous solution, interactions between the carbonyl portals of CB[6] and the ammonium groups of the guests are understood in terms of interactions with water molecules. However, in the gas phase, the conformational adjustment of the alkyl chain occurs from outside the CB[ $n$ ] portals to maximize ion–dipole interactions. As a result, TMD, which is completely trapped in the CB[6] cavity, forms the strongest complex in the gas phase. This finding indicates that the exceptionally strong binding of HMD with CB[6] in the solution is not solely due to the intrinsic properties of HMD and CB[6]. HMD requires a distortion in the conformation to maximize its binding to CB[6], whereas TMD does not, as indicated by the DFT calculations (Figure 4). Therefore, the exceptionally strong binding of HMD in aqueous solution can be explained by the presence of water molecules that can compensate for a relatively less rigid intrinsic Coulombic interaction between HMD and CB[6].

The thermodynamic values (Table 1) of the CB[7] complex formation with alkyldiammonium guests indicate that the high  $K_a$  is largely due to the higher entropic gain, which results from the less restricted motion of the guest in CB[7] than in CB[6]. MD simulations also show a much higher fluctuation of the guest in CB[7]. The average planar deviation of the guest from the center of CB[7] is approximately 1 Å, whereas the deviation of the guest in the CB[6] complex is approximately 0.5 Å (Table S3, Supporting Information). The packing coefficients of the CB[7]–alkyldiammonium complexes are approximately 35% (Table S4, Supporting Information), which are much lower than the ideal packing coefficient by Rebek's rule (approximately 55%).<sup>61</sup> Similar to the CB[6] complex system, weak interactions between CB[7] and alkyldiammonium cations are compensated by interactions with solvent water molecules (Figure 5). The blocking effect of the hydration layer around the CB[7] portals further prevents the refilling of the

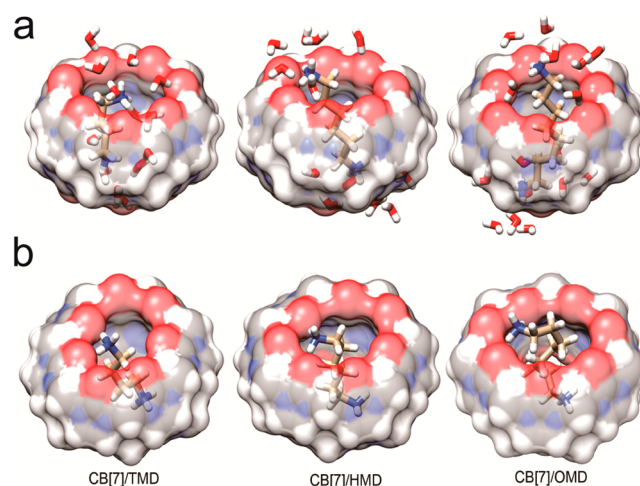


**Figure 5.** (a) The representative snapshots of CB[7]–TMD, CB[7]–HMD, and CB[7]–OMD from 10 ns MD simulations and (b) the structure of CB[7]–TMD, CB[7]–HMD, and CB[7]–OMD from DFT calculations. CB[7]–TMD does not form a stable inclusion complex in solution MD simulation, and the snapshot represents how water molecules start to enter the CB[7] cavity and interact with TMD.

larger cavity by water, similar to the role of the hydration shell in ligand–receptor binding.<sup>62</sup>

The absence of water molecules also affects the gas-phase stabilities of CB[7]–alkyldiammonium complex ions. Although the interaction between TMD and CB[7] is too weak to measure with ITC, the strongest gas-phase stability is observed among the CB[*n*] complex ions investigated in the present study. Our MD simulations also show that the complexation between CB[7] and TMD is unstable and that the displacement of TMD by water molecules occurs (Figure 5).

Although the packing coefficient of CB[7]–TMD is not determined because a stable complex is not formed in the MD simulations, the packing coefficient would be even smaller ( $\leq 30\%$ ) than the other CB[7] complexes. Because the CB[7] cavity is large enough to accept additional water molecules, even with TMD included, water molecules occupy the CB[7] cavity at the beginning of the simulation. TMD is then excluded to the aqueous phase. Subsequently, the entropic gain expected in CB[7]–TMD is insufficiently small, so the thermodynamic values cannot be obtained in our ITC experiments. However, in the absence of water solvent, the adequate length of TMD to the CB[7] height allows the guest to bind strongly to the host, similar to the host–guest chemistry with CB[6]. The finding that the stability of the complex is strongest in the gas phase indicates that the weak binding of TMD to CB[7] is not a sole intrinsic property between TMD and CB[7]. The interaction with solvent water is one of the key factors to the binding of guests to CB[*n*].

## CONCLUSIONS

Studies of the host–guest chemistry between a series of alkyldiammonium guests and CB[*n*] in solution and the gas phase reveal an additional role of the water solvent other than the conventional description of the host–guest binding event. Previous studies have focused more on the specific interaction between the host and the guest,<sup>7,25,26</sup> whereas our study shows that the high affinity binding is not an intrinsic property between only the host and the guest. The gas phase stabilities of CB[*n*]–alkyldiammonium complexes are dominated by the ion–dipole interactions and the conformational strain of the guest following the process. However, in the solution phase, the problem of the structurally unfavored interaction can be resolved by the solvent water, with which the guests prefer to form supplemental hydrogen bonds than endure distortion of the alkyl chain to maximize ion–dipole interactions. Additionally, the entropic gain from energetically guided complexation is dependent on whether there is enough free space for guests to share with water molecules. Our studies show that the conformation and the interaction of the host–guest system with the surroundings posterior to the complexation deserve to receive more attention for the interpretation of the binding event in the solution phase. We emphasize the importance of this often overlooked factor, and we believe that considering this factor would aid greatly in designing synthetic host–guest systems with higher binding affinities.

## ASSOCIATED CONTENT

### Supporting Information

ITC titration curves, ESI mass spectra, CID mass spectra, and TWIMS calibration curve for CB[*n*]–diammonium are given. Energy and structure-relevant values obtained from MD simulations are shown as tables. Additional experimental

methods are also included. This material is available free of charge via the Internet at <http://pubs.acs.org>.

## AUTHOR INFORMATION

### Corresponding Author

\*E-mail: [hughkim@postech.edu](mailto:hughkim@postech.edu).

### Notes

The authors declare no competing financial interest.

## ACKNOWLEDGMENTS

This work is supported by Basic Science Research (H.I.K.; Grant No. 2010-0021508) and World Class University (WCU) program (R31-10059) through the National Research Foundation (NRF) of Korea funded by the Ministry of Education, Science and Technology (MOEST). S.J.C.L. is supported by NRF Grant funded by the Korean Government (NRF-2011-Global Ph.D. Fellowship program). Partial support is provided by the Research Center Program (Project No. CA1203) of Institute for Basic Science (IBS) in Korea.

## REFERENCES

- (1) Oshovsky, G. V.; Reinhoudt, D. N.; Verboom, W. *Supramolecular Chemistry in Water*. *Angew. Chem., Int. Ed.* **2007**, *46*, 2366–2393.
- (2) Uhlenheuer, D. A.; Petkau, K.; Brunsveld, L. Combining Supramolecular Chemistry with Biology. *Chem. Soc. Rev.* **2010**, *39*, 2817–2826.
- (3) Mock, W. *Cucurbituril. Supramolecular Chemistry II — Host Design and Molecular Recognition*; Springer: Berlin/Heidelberg, Germany, 1995; p 1.
- (4) Lee, J. W.; Samal, S.; Selvapalam, N.; Kim, H. J.; Kim, K. Cucurbituril Homologues and Derivatives: New Opportunities in Supramolecular Chemistry. *Acc. Chem. Res.* **2003**, *36*, 621–630.
- (5) Lagona, J.; Mukhopadhyay, P.; Chakrabarti, S.; Isaacs, L. The Cucurbit[*n*]uril Family. *Angew. Chem., Int. Ed.* **2005**, *44*, 4844–4870.
- (6) Jeon, W. S.; Moon, K.; Park, S. H.; Chun, H.; Ko, Y. H.; Lee, J. Y.; Lee, E. S.; Samal, S.; Selvapalam, N.; Rekharsky, M. V.; et al. Complexation of Ferrocene Derivatives by the Cucurbit[7]uril Host: A Comparative Study of the Cucurbituril and Cyclodextrin Host Families. *J. Am. Chem. Soc.* **2005**, *127*, 12984–12989.
- (7) Kim, Y.; Kim, H.; Ko, Y. H.; Selvapalam, N.; Rekharsky, M. V.; Inoue, Y.; Kim, K. Complexation of Aliphatic Ammonium Ions with a Water-Soluble Cucurbit[6]uril Derivative in Pure Water: Isothermal Calorimetric, NMR, and X-ray Crystallographic Study. *Chem.—Eur. J.* **2009**, *15*, 6143–6151.
- (8) Biedermann, F.; Uzunova, V. D.; Scherman, O. A.; Nau, W. M.; De Simone, A. Release of High-Energy Water as an Essential Driving Force for the High-Affinity Binding of Cucurbit[*n*]urils. *J. Am. Chem. Soc.* **2012**, *134*, 15318–15323.
- (9) Buschmann, H. J.; Jansen, K.; Schollmeyer, E. Cucurbituril as Host Molecule for the Complexation of Aliphatic Alcohols, Acids and Nitriles in Aqueous Solution. *Thermochim. Acta* **2000**, *346*, 33–36.
- (10) Rekharsky, M. V.; Yamamura, H.; Inoue, C.; Kawai, M.; Osaka, I.; Arakawa, R.; Shiba, K.; Sato, A.; Ko, Y. H.; Selvapalam, N.; Kim, K.; Inoue, Y. Chiral Recognition in Cucurbituril Cavities. *J. Am. Chem. Soc.* **2006**, *128*, 14871–14880.
- (11) Nau, W. M.; Ghale, G.; Hennig, A.; Bakirci, H.; Bailey, D. M. Substrate-Selective Supramolecular Tandem Assays: Monitoring Enzyme Inhibition of Arginase and Diamine Oxidase by Fluorescent Dye Displacement from Calixarene and Cucurbituril Macrocycles. *J. Am. Chem. Soc.* **2009**, *131*, 11558–11570.
- (12) Gomez-Casado, A.; Jonkheijm, P.; Huskens, J. Recognition Properties of Cucurbit[7]uril Self-Assembled Monolayers Studied with Force Spectroscopy. *Langmuir* **2011**, *27*, 11508–11513.
- (13) Minami, T.; Esipenko, N. A.; Zhang, B.; Isaacs, L.; Nishiyabu, R.; Kubo, Y.; Anzenbacher, P. Supramolecular Sensor for Cancer-Associated Nitrosamines. *J. Am. Chem. Soc.* **2012**, *134*, 20021–20024.



- (14) Li, H.; Xie, H. N.; Cao, Y.; Ding, X. R.; Yin, Y. M.; Li, G. X. A General Way to Assay Protein by Coupling Peptide with Signal Reporter via Supramolecule Formation. *Anal. Chem.* **2013**, *85*, 1047–1052.
- (15) Ko, Y. H.; Kim, E.; Hwang, I.; Kim, K. Supramolecular Assemblies Built with Host-Stabilized Charge-Transfer Interactions. *Chem. Commun.* **2007**, 1305–1315.
- (16) Kim, K. Mechanically Interlocked Molecules Incorporating Cucurbituril and Their Supramolecular Assemblies. *Chem. Soc. Rev.* **2002**, *31*, 96–107.
- (17) Lim, Y.-b.; Kim, T.; Lee, J. W.; Kim, S.-m.; Kim, H.-J.; Kim, K.; Park, J.-s. Self-Assembled Ternary Complex of Cationic Dendrimer, Cucurbituril, and DNA: Noncovalent Strategy in Developing a Gene Delivery Carrier. *Bioconjugate Chem.* **2002**, *13*, 1181–1185.
- (18) Kim, S. K.; Park, K. M.; Singha, K.; Kim, J.; Ahn, Y.; Kim, K.; Kim, W. J. Galactosylated Cucurbituril-Inclusion Polyplex for Hepatocyte-Targeted Gene Delivery. *Chem. Commun.* **2010**, *46*, 692–694.
- (19) Park, K. M.; Lee, D.-W.; Sarkar, B.; Jung, H.; Kim, J.; Ko, Y. H.; Lee, K. E.; Jeon, H.; Kim, K. Reduction-Sensitive, Robust Vesicles with a Non-Covalently Modifiable Surface as a Multifunctional Drug-Delivery Platform. *Small* **2010**, *6*, 1430–1441.
- (20) Bush, M. E.; Bouley, N. D.; Urbach, A. R. Charge-Mediated Recognition of N-Terminal Tryptophan in Aqueous Solution by a Synthetic Host. *J. Am. Chem. Soc.* **2005**, *127*, 14511–14517.
- (21) Reczek, J. J.; Kennedy, A. A.; Halbert, B. T.; Urbach, A. R. Multivalent Recognition of Peptides by Modular Self-Assembled Receptors. *J. Am. Chem. Soc.* **2009**, *131*, 2408–2415.
- (22) Urbach, A. R.; Ramalingam, V. Molecular Recognition of Amino Acids, Peptides, and Proteins by Cucurbit[n]uril Receptors. *Isr. J. Chem.* **2011**, *51*, 664–678.
- (23) Chinai, J. M.; Taylor, A. B.; Ryno, L. M.; Hargreaves, N. D.; Morris, C. A.; Hart, P. J.; Urbach, A. R. Molecular Recognition of Insulin by a Synthetic Receptor. *J. Am. Chem. Soc.* **2011**, *133*, 8810–8813.
- (24) Kellersberger, K. A.; Anderson, J. D.; Ward, S. M.; Krakowiak, K. E.; Dearden, D. V. Encapsulation of N<sub>2</sub>, O<sub>2</sub>, Methanol, or Acetonitrile by Decamethylcucurbit[5]uril(NH<sub>4</sub><sup>+</sup>)<sub>2</sub> Complexes in the Gas Phase: Influence of the Guest on “Lid” Tightness. *J. Am. Chem. Soc.* **2001**, *123*, 11316–11317.
- (25) Mock, W. L.; Shih, N. Y. Host-Guest Binding Capacity of Cucurbituril. *J. Org. Chem.* **1983**, *48*, 3618–3619.
- (26) Mock, W. L.; Shih, N. Y. Structure and Selectivity in Host-Guest Complexes of Cucurbituril. *J. Org. Chem.* **1986**, *51*, 4440–4446.
- (27) Freeman, W. A.; Mock, W. L.; Shih, N. Y. Cucurbituril. *J. Am. Chem. Soc.* **1981**, *103*, 7367–7368.
- (28) Moghaddam, S.; Yang, C.; Rekharsky, M.; Ko, Y. H.; Kim, K.; Inoue, Y.; Gilson, M. K. New Ultrahigh Affinity Host-Guest Complexes of Cucurbit[7]uril with Bicyclo[2.2.2]octane and Adamantane Guests: Thermodynamic Analysis and Evaluation of M2 Affinity Calculations. *J. Am. Chem. Soc.* **2011**, *133*, 3570–3581.
- (29) Rekharsky, M. V.; Mori, T.; Yang, C.; Ko, Y. H.; Selvapalam, N.; Kim, H.; Sobransingh, D.; Kaifer, A. E.; Liu, S.; Isaacs, L.; et al. A Synthetic Host-Guest System Achieves Avidin-Biotin Affinity by Overcoming Enthalpy–Entropy Compensation. *Proc. Natl. Acad. Sci. U.S.A.* **2007**, *104*, 20737–20742.
- (30) Osaka, I.; Kondou, M.; Selvapalam, N.; Samal, S.; Kim, K.; Rekharsky, M. V.; Inoue, Y.; Arakawa, R. Characterization of Host-Guest Complexes of Cucurbit[n]uril (*n* = 6, 7) by Electrospray Ionization Mass Spectrometry. *J. Mass Spectrom.* **2006**, *41*, 202–207.
- (31) Zhang, H.; Ferrell, T. A.; Asplund, M. C.; Dearden, D. V. Molecular Beads on a Charged Molecular String:  $\alpha,\omega$ -Alkyldiammonium Complexes of Cucurbit[6]uril in the Gas Phase. *Int. J. Mass Spectrom.* **2007**, *265*, 187–196.
- (32) Zhang, H.; Paulsen, E. S.; Walker, K. A.; Krakowiak, K. E.; Dearden, D. V. Cucurbit[6]uril Pseudorotaxanes: Distinctive Gas-Phase Dissociation and Reactivity. *J. Am. Chem. Soc.* **2003**, *125*, 9284–9285.
- (33) Dearden, D. V.; Ferrell, T. A.; Asplund, M. C.; Zilch, L. W.; Julian, R. R.; Jarrold, M. F. One Ring to Bind Them All: Shape-Selective Complexation of Phenylenediamine Isomers with Cucurbit[6]uril in the Gas Phase. *J. Phys. Chem. A* **2009**, *113*, 989–997.
- (34) Zhang, H.; Grabenauer, M.; Bowers, M. T.; Dearden, D. V. Supramolecular Modification of Ion Chemistry: Modulation of Peptide Charge State and Dissociation Behavior through Complexation with Cucurbit[n]uril (*n* = 5, 6) or  $\alpha$ -Cyclodextrin. *J. Phys. Chem. A* **2009**, *113*, 1508–1517.
- (35) Deroo, S.; Rauwald, U.; Robinson, C. V.; Scherman, O. A. Discrete, Multi-Component Complexes with Cucurbit[8]uril in the Gas-Phase. *Chem. Commun.* **2009**, 644–646.
- (36) Rauwald, U.; Biedermann, F.; Deroo, S.; Robinson, C. V.; Scherman, O. A. Correlating Solution Binding and ESI-MS Stabilities by Incorporating Solvation Effects in a Confined Cucurbit[8]uril System. *J. Phys. Chem. B* **2010**, *114*, 8606–8615.
- (37) Yang, F.; Dearden, D. V. Gas Phase Cucurbit[n]uril Chemistry. *Isr. J. Chem.* **2011**, *51*, 551–558.
- (38) Heo, S. W.; Choi, T. S.; Park, K. M.; Ko, Y. H.; Kim, S. B.; Kim, K.; Kim, H. I. Host-Guest Chemistry in the Gas Phase: Selected Fragmentations of CB[6]-Peptide Complexes at Lysine Residues and Its Utility to Probe the Structures of Small Proteins. *Anal. Chem.* **2011**, *83*, 7916–7923.
- (39) Cernochova, J.; Branna, P.; Rouchal, M.; Kulhanek, P.; Kuritka, I.; Vicha, R. Determination of Intrinsic Binding Modes by Mass Spectrometry: Gas-Phase Behavior of Adamantylated Bisimidazolium Guests Complexed to Cucurbiturils. *Chem.—Eur. J.* **2012**, *18*, 13633–13637.
- (40) Mitkina, T.; Fedin, V.; Llusar, R.; Sorribes, I.; Vicent, C. Distinctive Unimolecular Gas-Phase Reactivity of [M(en)<sub>2</sub>]<sup>2+</sup> (M=Ni, Cu) Dications and Their Inclusion Complexes with the Macrocyclic Cavitand Cucurbit[8]uril. *J. Am. Soc. Mass Spectrom.* **2007**, *18*, 1863–1872.
- (41) Choi, T. S.; Ko, J. Y.; Heo, S. W.; Ko, Y. H.; Kim, K.; Kim, H. I. Unusual Complex Formation and Chemical Reaction of Haloacetate Anion on the Exterior Surface of Cucurbit[6]uril in the Gas Phase. *J. Am. Soc. Mass Spectrom.* **2012**, *23*, 1786–1793.
- (42) Lee, T.-C.; Kalenius, E.; Lazar, A. I.; Assaf, K. I.; Kuhnert, N.; Grün, C. H.; Jänis, J.; Scherman, O. A.; Nau, W. M. Chemistry inside Molecular Containers in the Gas Phase. *Nat. Chem.* **2013**, *5*, 376–382.
- (43) Lee, J. W.; Heo, S. W.; Lee, S. J. C.; Ko, J. Y.; Kim, H.; Kim, H. I. Probing Conformational Changes of Ubiquitin by Host-Guest Chemistry Using Electrospray Ionization Mass Spectrometry. *J. Am. Soc. Mass Spectrom.* **2013**, *24*, 21–29.
- (44) Becke, A. D. Density-Functional Thermochemistry. III. The Role of Exact Exchange. *J. Chem. Phys.* **1993**, *98*, 5648–5652.
- (45) Shao, Y.; Fusti-Molnar, L.; Jung, Y.; Kussmann, J.; Ochsenfeld, C.; Brown, S. T.; Gilbert, A. T. B.; Slipchenko, L. V.; Levchenko, S. V.; O'Neill, D. P.; et al. Advances in Methods and Algorithms in a Modern Quantum Chemistry Program Package. *Phys. Chem. Chem. Phys.* **2006**, *8*, 3172–3191.
- (46) Lee, C. T.; Yang, W. T.; Parr, R. G. Development of the Colle-Salvetti Correlation-Energy Formula into a Functional of the Electron-Density. *Phys. Rev. B* **1988**, *37*, 785–789.
- (47) Harihara, P. C.; Pople, J. A. Effect of D-Functions on Molecular-Orbital Energies for Hydrocarbons. *Chem. Phys. Lett.* **1972**, *16*, 217–219.
- (48) Rassolov, V. A.; Pople, J. A.; Ratner, M. A.; Windus, T. L. *J. Chem. Phys.* **1998**, *109*, 1223.
- (49) Rassolov, V. A.; Pople, J. A.; Ratner, M. A.; Windus, T. L. 6-31G\* Basis Set for Atoms K through Zn. *J. Chem. Phys.* **1998**, *109*, 1223–1229.
- (50) Hess, B.; Kutzner, C.; van der Spoel, D.; Lindahl, E. GROMACS 4: Algorithms for Highly Efficient, Load-Balanced, and Scalable Molecular Simulation. *J. Chem. Theory Comput.* **2008**, *4*, 435–447.
- (51) Hornak, V.; Abel, R.; Okur, A.; Strockbine, B.; Roitberg, A.; Simmerling, C. Comparison of Multiple Amber Force Fields and

Development of Improved Protein Backbone Parameters. *Proteins* **2006**, *65*, 712–725.

(52) Nau, W. M.; Florea, M.; Assaf, K. I. Deep inside Cucurbiturils: Physical Properties and Volumes of Their Inner Cavity Determine the Hydrophobic Driving Force for Host-Guest Complexation. *Isr. J. Chem.* **2011**, *51*, 559–577.

(53) Darden, T.; York, D.; Pedersen, L. Particle Mesh Ewald: An  $N \log(N)$  Method for Ewald Sums in Large Systems. *J. Chem. Phys.* **1993**, *98*, 10089–10092.

(54) Berendsen, H. J. C.; Postma, J. P. M.; Gunsteren, W. F. v.; DiNola, A.; Haak, J. R. Molecular Dynamics with Coupling to an External Bath. *J. Chem. Phys.* **1984**, *81*, 3684–3690.

(55) Rekharsky, M. V.; Ko, Y. H.; Selvapalam, N.; Kim, K.; Inoue, Y. Complexation Thermodynamics of Cucurbit[6]uril with Aliphatic Alcohols, Amines, and Diamines. *Supramol. Chem.* **2007**, *19*, 39–46.

(56) Liu, S.; Ruspici, C.; Mukhopadhyay, P.; Chakrabarti, S.; Zavalij, P. Y.; Isaacs, L. The Cucurbit[*n*]uril Family: Prime Components for Self-Sorting Systems. *J. Am. Chem. Soc.* **2005**, *127*, 15959–15967.

(57) Daniel, J. M.; Friess, S. D.; Rajagopalan, S.; Wendt, S.; Zenobi, R. Quantitative Determination of Noncovalent Binding Interactions Using Soft Ionization Mass Spectrometry. *Int. J. Mass Spectrom.* **2002**, *216*, 1.

(58) Thalassinou, K.; Grabenauer, M.; Slade, S. E.; Hilton, G. R.; Bowers, M. T.; Scrivens, J. H. Characterization of Phosphorylated Peptides Using Traveling Wave-Based and Drift Cell Ion Mobility Mass Spectrometry. *Anal. Chem.* **2009**, *81*, 248–254.

(59) Israelachvili, J.; Wennerstrom, H. Role of Hydration and Water Structure in Biological and Colloidal Interactions. *Nature* **1996**, *379*, 219–225.

(60) Raschke, T. M. Water Structure and Interactions with Protein Surfaces. *Curr. Opin. Struct. Biol.* **2006**, *16*, 152–159.

(61) Mecozzi, S.; Rebek, J. The 55% Solution: A Formula for Molecular Recognition in the Liquid State. *Chem.—Eur. J.* **1998**, *4*, 1016–1022.

(62) Scorciapino, M. A.; Robertazzi, A.; Casu, M.; Ruggerone, P.; Ceccarelli, M. Heme Proteins: The Role of Solvent in the Dynamics of Gates and Portals. *J. Am. Chem. Soc.* **2010**, *132*, 5156–5163.